Supporting Information

Fabrication of Water-Resistant Fluorescent Ink by Near-Unity Photoluminescence Quantum yield of Doped $CsPbBr_3$ via $NiBr_2$

Dipanwita Roy, [a] Shramana Guha[a] and Somobrata Acharya*[a,b]

[a] School of Applied and Interdisciplinary Sciences, Indian Association for the Cultivation of Science, Jadavpur, Kolkata 700032 (India).

[b] Technical Research Centre, Indian Association for the Cultivation of Science, Jadavpur, Kolkata700032 (India).

Corresponding Author: camsa2@iacs.res.in

Contents:

Supporting Figures

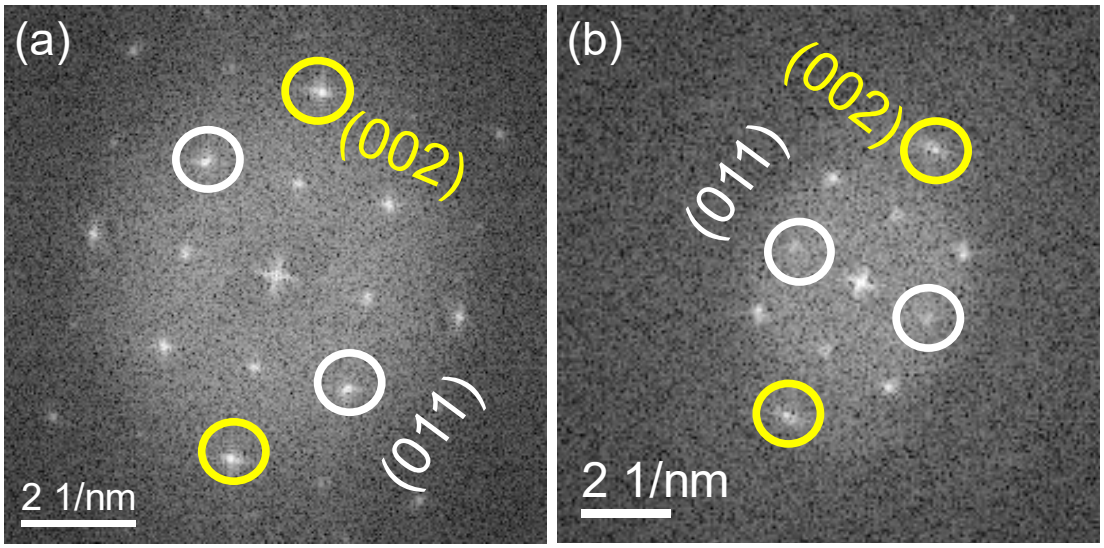

Fig. S1 FFT patterns of (a) $CsPbBr_3$ NCs (b) Ni^{2+} doped $CsPbBr_3$ NCs showing spots corresponding to (011) and (002) planes.

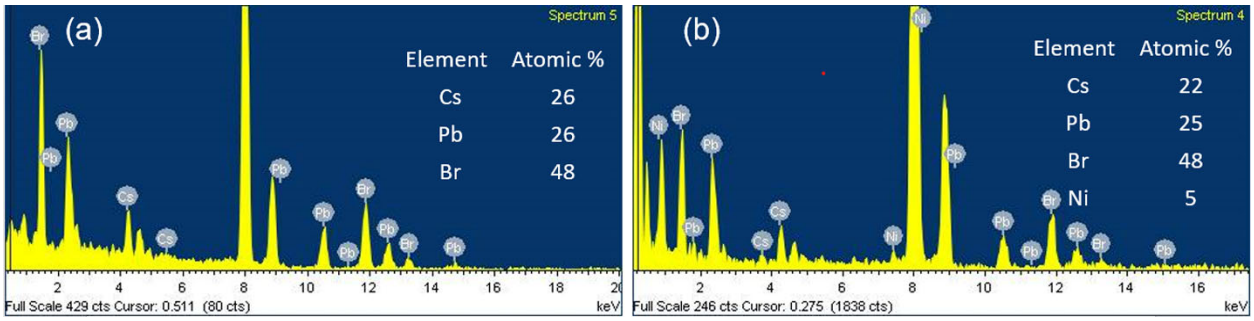

Fig. S2 (a-b) EDX showing the constituent elements of $CsPbBr_3$ NCs and Ni^{2+} doped $CsPbBr_3$ NCs. Insets show the atomic percentage of the elements confirming the effective doping of Ni^{2+} in $CsPbBr_3$ NCs. The EDX shown in right panel corresponds to Ni/Pb ratio of 0.34 (corresponding Ni/Pb molar ratio used in synthesis is 0.5).

Ni/Pb Elemental Ratio (from ICP)	*Ni/Pb Molar Ratio Used in the Synthesis*
0	0
0.075	0.1
0.18	0.25
0.26	0.35
0.38	**0.5**
0.53	0.7

Table S1. Ni/Pb molar ratio used in the synthesis for the variation of Ni dopant concentration and the elemental ratio measured using ICP-AES showing Ni-incorporation in $CsPbBr_3$ NCs.

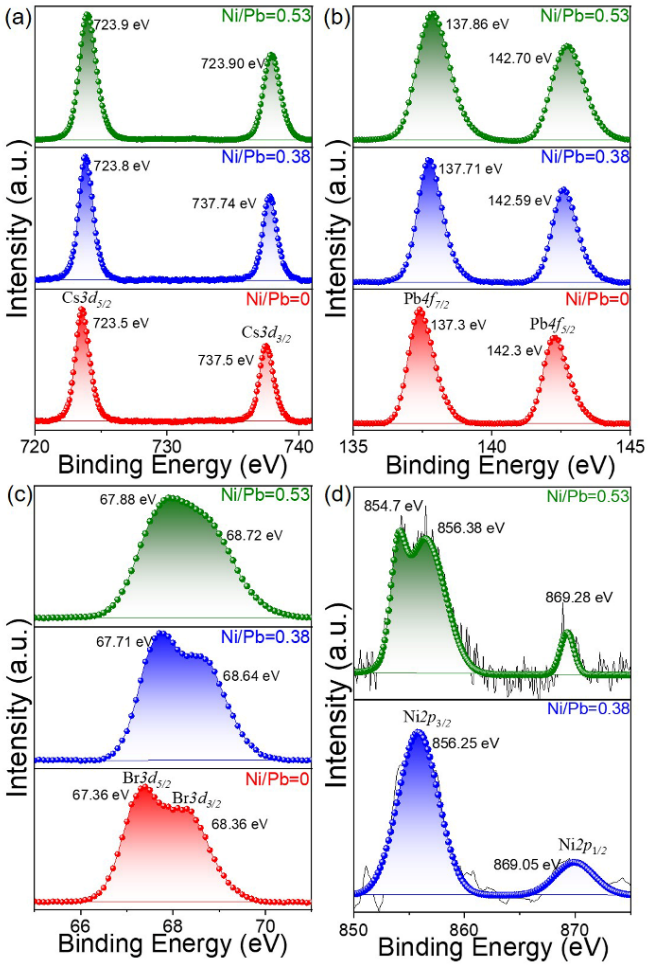

Fig. S3 XPS spectra for $CsPbBr_3$ NCs (red, Ni/Pb=0) and Ni^{2+} doped $CsPbBr_3$ NCs (blue, Ni/Pb=0.38 and green, Ni/Pb=0.53) showing the change in octahedral environment upon increasing Ni^{2+} concentration. The Ni/Pb ratio from ICP-AES is used in legends. For Ni/Pb=0.53,

an additional peak for Ni *2p* appears at ~854.7 eV due to the surface Ni-O bonds which may relate to the bonding between surface Ni^{2+} and ligands.[1]

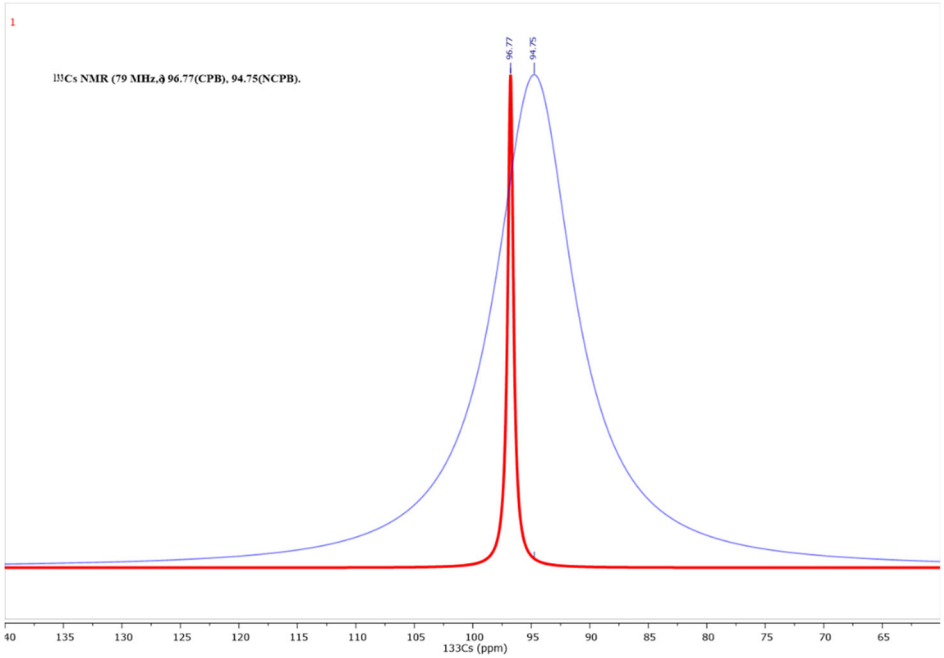

Fig. S4 ^{133}Cs NMR spectra for both $CsPbBr_3$ (red line) and Ni^{2+} doped $CsPbBr_3$ (blue line) NCs showing change in local environment of $[PbBr_6]^{4-}$ octahedra upon Ni^{2+} incorporation in $CsPbBr_3$ NCs.

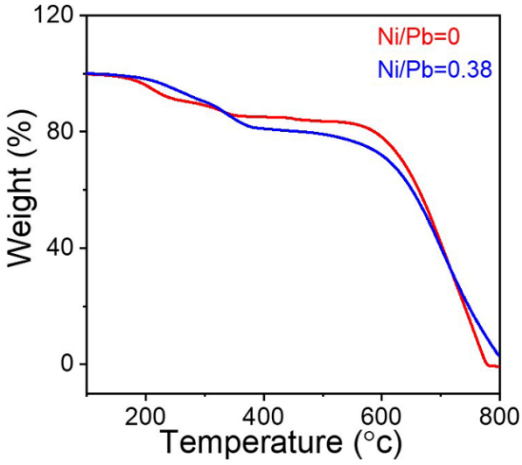

Fig. S5 TGA curves for both $CsPbBr_3$ (red line) and Ni^{2+} doped $CsPbBr_3$ (blue line) NCs showing extent of thermal stability.

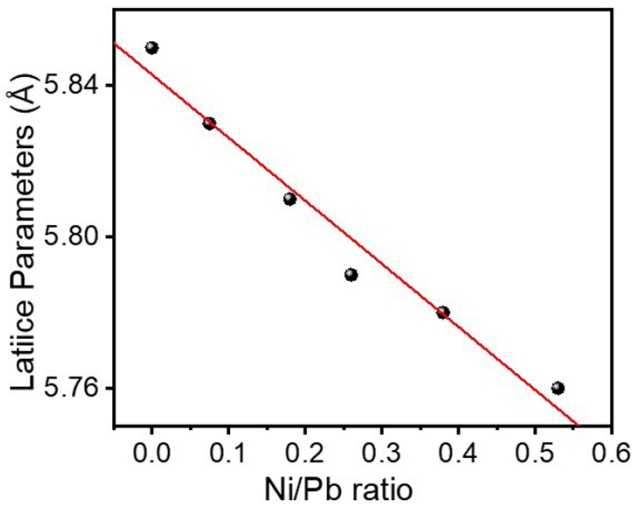

Fig. S6 Lattice parameters versus Ni/Pb elemental ratio (obtained from ICP-AES) shows linear relationship.

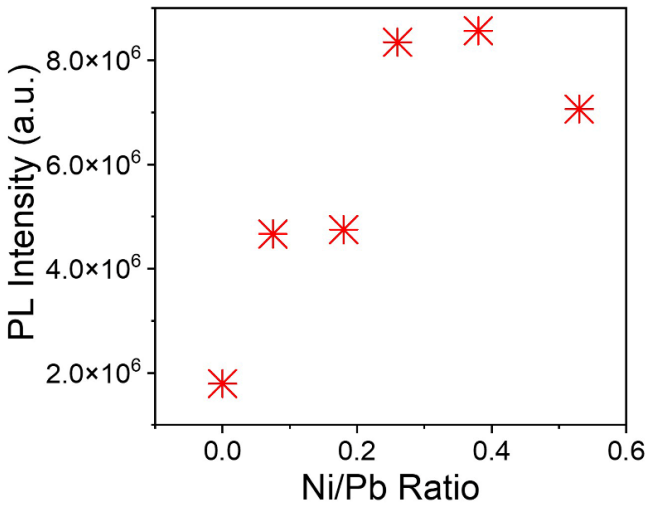

Fig. S7 Variation of PL intensity with changing the Ni/Pb elemental ratio (obtained from ICP-AES).

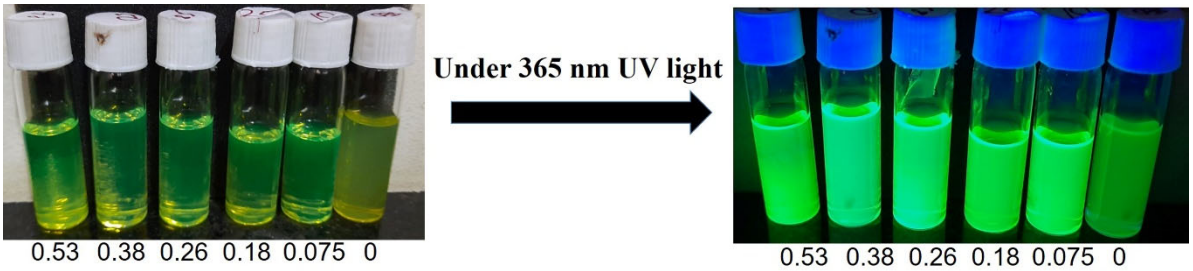

Fig. S8 The images of the doped and undoped $CsPbBr_3$ NCs in hexane with changing Ni/Pb elemental ratio (obtained from ICP-AES).

Ni/Pb Elemental Ratio (from ICP-AES)	*Ni/Pb Molar ratio used in the synthesis*	*PLQY (%)*
0	0	68
0.075	0.1	72
0.18	0.25	78
0.26	0.35	81
0.38	**0.5**	**98**
0.53	0.7	72

Table S2. Comparison of PLQY with increasing dopant concentration measured from ICP-AES and Ni/Pb molar ratio used in the synthesis.

Literature	**Material**	**PLQY**	**Ni Concentration**
2	Ni^{2+} doped $CsPbCl_3$	96.5%	11.9%
	Ni^{2+}doped $CsPbCl_{2.4}Br_{0.6}$	92%	2.8%
	Ni^{2+} doped $CsPbCl_2Br$	93%	2.2%
3	Ni^{2+} doped $CsPbCl_3$	72%	6.1% Ni
	Ni^{2+} and Pr^{3+} doped $CsPbCl_3$	89%	
4	Ni^{2+} doped $CsPbBr_3$	82.9%	Feed molar ratio Ni/Pb=2.5
5	Ni^{2+} doped $CsPbBr_3$ powder	39.27%	8.5%
6	Ni^{2+} doped $CsPbBr_3$ nanoplatelets	78%	From Ni-Br mixed solution (0.2 mmol $NiBr_2$ in 0.2 ml HBr) 0.35 μL used
7	Ni^{2+} doped $CsPbBr_3$ nanocrystals	Not available	-
8	Ni^{2+} doped $CsPbBr_3$ quantum dots	70.62%	22%
		90.77%	after $Pb_3(PO4)_2$ coating
Our work	**Ni^{2+} doped $CsPbBr_3$ nanocrystals**	**98%**	**~5.6%**

Table S3. Comparison of PLQY with dopant (Ni^{2+}) concentration obtained from literatures. [2–8]

Ni/Pb Elemental Ratio (from ICP-AES)	τ_1 *(ns)*	τ_2 *(ns)*	τ_3 *(ns)*	A_1	A_2	A_3	τ_{avg}*(ns)*
0	11.6	61.0	2.6	0.20	0.02	0.78	5.4
0.075	8.7	3.9	34.0	0.30	0.67	0.03	5.4
0.18	7.8	2.2	32.2	0.25	0.02	0.73	4.8
0.26	6.7	23.6	2.0	0.29	0.03	0.68	4.6
0.38	**5.1**	**1.4**	**15.9**	**0.5**	**0.4**	**0.09**	**4.0**
0.53	10.5	38.6	3.1	0.24	0.02	0.74	5.6

Table S4. Time-resolved photoluminescence decay parameters of the $CsPbBr_3$ and Ni^{2+} doped $CsPbBr_3$ NCs while varying the amount of dopant.

Ni/Pb Elemental Ratio (from ICP-AES)	$K_r(s^{-1})\times 10^9$	$K_{nr}(s^{-1})\times 10^9$
0	0.125	0.185
0.075	0.133	0.052
0.18	0.1625	0.0458
0.26	0.2025	0.0475
0.38	0.213	0.0044
0.53	0.128	0.05

Table S5. Radiative (K_r) and non-radiative (K_{nr}) decay rate of the $CsPbBr_3$ and Ni^{2+} doped $CsPbBr_3$ NCs while varying dopant concentration.

**Equation 1,2 have been followed to calculate the Radiative (K_r) and non-radiative (K_{nr}) decay rates:*

$k_{tot} = k_{nr} + k_r = 1/\tau_{avg}$ .....(equation 1); $k_r = PLQY/\tau_{avg}$ ... ... (equation 2)

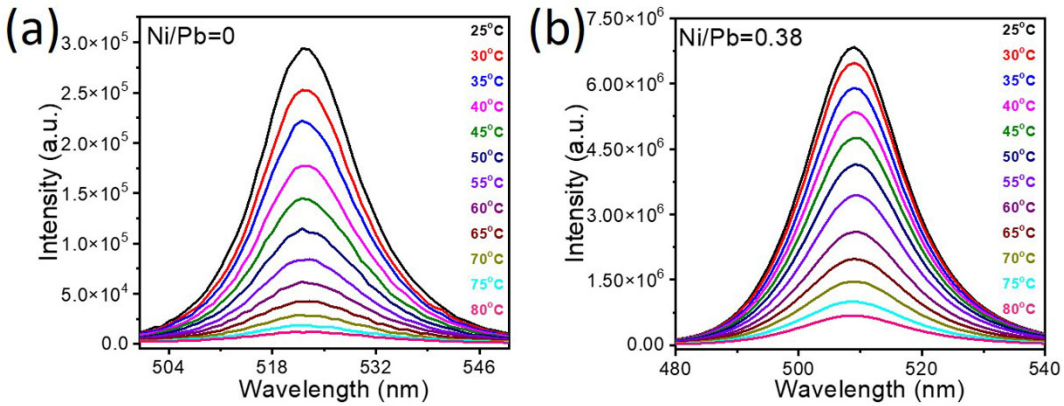

Fig. S9 (a-b) Temperature dependent PL confirming the trends in reduction of PL with temperature is similar with the luminescent ink. The extent of drop of PL is maximized for pristine one compared to the doped $CsPbBr_3$ NCs (elemental ratio of Ni/Pb=0.38). This observation supports the fact that Ni^{2+} doped $CsPbBr_3$ NCs show enhanced temperature stability.

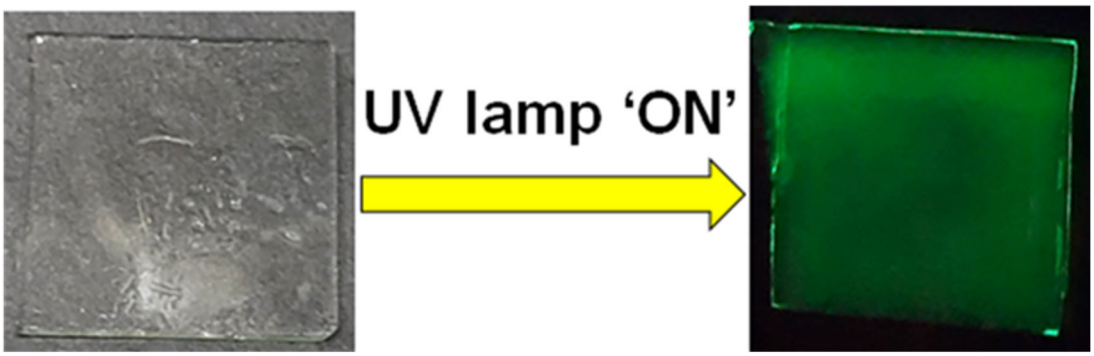

Fig. S10 The thin glass-film of the fluorescent ink placed on paper shows its transparency (left-side). The right-side image shows the luminescence nature of the thin film under the UV light illumination at 365 nm after several heating-cooling cycles.

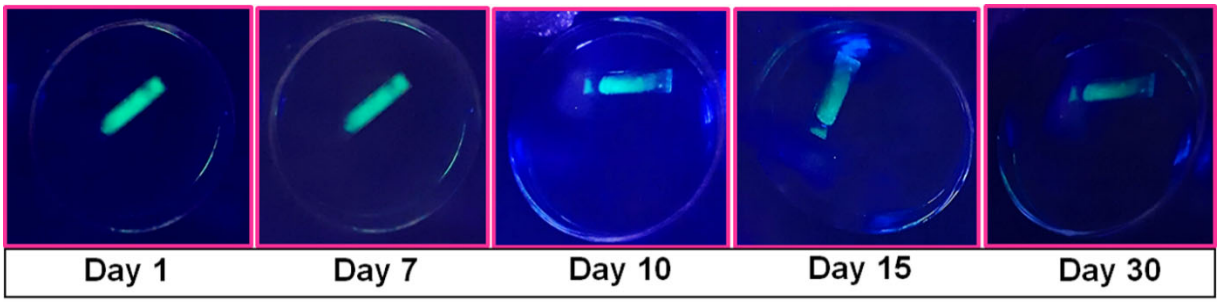

Fig. S11 Images of luminescence of the thin film of the fluorescent ink stored in water for several days (under UV light illumination).

References:

1 A. Shapiro, M. W. Heindl, F. Horani, M.-H. Dahan, J. Tang, Y. Amouyal and E. Lifshitz, *J. Phys. Chem. C*, 2019, **123**, 24979–24987.

2 Z.-J. Yong, S.-Q. Guo, J.-P. Ma, J.-Y. Zhang, Z.-Y. Li, Y.-M. Chen, B.-B. Zhang, Y. Zhou, J. Shu, J.-L. Gu, L.-R. Zheng, O. M. Bakr and H.-T. Sun, *J. Am. Chem. Soc.*, 2018, **140**, 9942–9951.

3 J. Lyu, B. Dong, G. Pan, L. Sun, X. Bai, S. Hu, B. Shen, B. Zhou, L. Wang, W. Xu, D. Zhou, L. Xu and H. Song, *Nanoscale*, 2021, **13**, 16598–16607.

4 H. Kim, S.-R. Bae, T. H. Lee, H. Lee, H. Kang, S. Park, H. W. Jang and S. Y. Kim, *Adv. Funct. Mater.*, 2021, **31**, 2102770.

5 T. Chen, R. Liu, S. Tang, X. Li, S. Ye, X. Duan, R. Wang, Y. Shi, J. Yang, F. Qiu, Y. Yang, X. Wen and C. Wang, *AIP Adv.*, 2021, **11**, 115008.

6 J. Song, Y. Gao, Z. Meng, Z. Jiang, X. Cao, Q. Zeng and T. Hu, *Opt. Mater. (Amst).*, 2023, **138**, 113611.

7 S. Thawarkar, P. J. S. Rana, R. Narayan and S. P. Singh, *Langmuir*, 2019, **35**, 17150–17155.

8 D. Huang, J. Bo, R. Zheng, C. Luo, X. Sun, Q. Li, D. Shen, Z. Zheng, M. Chen, Y. Yang, A. Tang, S. Chen and Y. Chen, *Adv. Opt. Mater.*, 2021, **9**, 2100474.